Scholar Publishing Group
International Journal of Multimedia Computing
https://doi.org/10.38007/IJMC.2020.010106
ISSN 2789-7168 Vol. 1, Issue 1: 74-88

Positioning Technology of Tiny Electronic Components Based on Microscope and Computer Vision

Peng Liu*

Xi'an Jiaotong University, Xi'an, China

PengLiu@xjtu.edu.cn

corresponding author

Keywords: Computer Vision, Industrial Microscope, Precision Positioning, Target Approach

Abstract: In recent years, with the rapid development of tiny electronic components. At present, commonly used optical inspection technology and electron microscope inspection technology find it difficult to meet the dimensional inspection requirements of key components of highly integrated integrated circuits. Based on computer micro-vision technology, the coupling of measuring platform displacement to the development of miniature electronic components is of great significance for the analysis and design of precision platforms. This paper analyzes the influence of the three factors of material, software and environment on the accuracy positioning of the measurement system. The analysis shows that the characteristics of the imaging system itself and the image noise it brings are the main factors that affect the measurement accuracy. In this paper, a technique for blindly detecting the position of the scanner based on computer vision is proposed. This article uses a CCD optical camera to capture the orbital motion of the electronic pen, and uses video image processing algorithms, computer vision and position to capture the position of the light on the screen. With the support of specific software, this article creates a new interactive whiteboard system. Any large screen can be turned into a large touch screen with electronic writing surface and touch function. The device does not require a specific additional screen to operate, and the cost is lower. In this paper, the stereo microscope has a narrow field of view, small depth of field and many non-linear factors. Based on the analysis of existing camera models, a binocular microscope imaging model based on a linear camera is established. On this basis, through the experimental analysis of the feasibility of the existing camera calibration method in the binocular microsystem, the calibration method of the camera's main parameters is proposed. Experiments show that the resolution value of the peak value of the evaluation curve in this paper is 18 times the focus resolution value, while the commonly used algorithm for evaluating the peak value of the curve is only 14 times. Compared with the latter, the discrimination of the edge gradient Laplacian used in this paper is more obvious than the former.

Copyright: © 2020 by the authors. This is an Open Access article distributed under the Creative Commons Attribution License (CC BY 4.0), which permits unrestricted use, distribution, and reproduction in any medium, provided the original work is properly cited (https://creativecommons.org/licenses/by/4.0/).

1. Introduction

Computer vision positioning technology is a detection method that combines digital image processing, optical principles, information processing knowledge and other scientific technologies into one. First, the test system collects the image of the researched object, extracts useful information from the picture, and then judges whether the researched object meets the test requirements based on the existing prior knowledge. The non-contact, real-time, flexibility and accuracy characteristics of this technology play an important role in the development of high-precision measurement technology. It is unmatched by traditional detection methods and shows a strong vitality in practice.

Based on the characteristics of the BGA chip, Han introduced a binocular single camera imaging welding positioning system based on computer vision technology. It describes the composition and principle of a single CCD vision system, and uses classic operators and gray system theory to process BGA chips with images. Experimental results show that the gray system theory is effective, has the function of an adjustable edge detection algorithm, and can more accurately detect the edges of useful information. Has a certain anti-noise ability, can effectively improve the positioning accuracy of BGA chips [1]. Cao inputs the coordinate of the feature point image into the calibrated system to obtain the actual coordinate of the feature point. The present invention solves the measurement problem caused by the problem of small target area to be measured, high positioning accuracy requirements, non-contact and other problems. The non-contact measurement method of microscopic stereo vision has achieved the precise positioning of precision parts [2]. Sharov uses a binocular microscopic stereo vision system, which uses two CCD cameras to collect the image of the tested part. The stereo microscope magnifies the image information of the area to be tested on the tested part; the two CCD cameras are calibrated using a checkerboard calibration plate; Harris corner detection algorithm and sub-pixel extraction algorithm are used to extract feature points. The extracted feature points are corrected for initial matching and matching point pairs [3].

In the research of computer vision positioning technology, the use of atomic force microscopy is a good method to solve many problems, so it is widely used in the research of computer vision positioning technology, such as the XE-3DM atomic force microscope invented by Zhang Using the corresponding mechanical structure, the AFM scanning probe is driven to perform oblique scanning according to the surface morphology of the scanned sample to obtain the side wall information of the sample. This method has extremely high requirements on the mechanical structure and is difficult to implement. It realizes the automatic loading and unloading of scanned samples through a manipulator. The AFM indirectly realizes the automatic replacement of the AFM scanning probe by replacing the probe holder equipped with the scanning probe [4].

This article introduces a blind spot detection technique for scanning the probe tip. This technology can convert the optical coordinates of the optical microscope and the coordinates of the AFM scanning platform, blindly place the tip of the scanning detector, and determine the position of the terminal coordinates of the AFM scanning detector in the optical coordinate system. Intuitively record the target point of the scanned sample and move the target scan point to the edge of the scan detector by transforming the coordinated sample and visual coordinates. To evaluate the camera of the experimental measurement system, this paper uses a calibrated camera model to perform a three-dimensional reconstruction experiment on the space points provided by the calibration board, and compares it with the ideal point and analyzes the error. It can be seen from the analysis that at a specific magnification, the horizontal calibration accuracy of the calibration method proposed in this paper is lower than the longitudinal calibration accuracy. The calibration accuracy is lower than this accuracy, which can meet the optical measurement requirements of the stereo microscope on the CNC processing platform.

2. Research on Positioning Technology of Tiny Electronic Components Based on Microscope and Computer Vision

2.1. AFM Probe Automatic Approach Method Research

This paper studies AFM automatic approach and proposes an automatic approach based on computer vision and AFM accurate force feedback technology. This method accomplishes the automatic approximation of the scanning probe through the segmented approximation combined with coarse and fine [5].

(1) Image sharpness evaluation function

In this paper, the Laplce operator which has an enhanced effect on the image edge is selected for research. The Laplce operator is a second-order differential operator defined in N-dimensional Euclidean space, which has isotropy and rotation invariance, thus meeting the sharpening requirements of image edges with different directions, and can be used as a higher-order component of the image Estimate. In the field of image processing, it is widely used in image edge extraction, image edge sharpening, and camera focusing [6-7].

The classical Laplace operator is defined as:

$$\nabla^2 f(x,y) = \frac{\partial^2 f}{\partial x^2} + \frac{\partial^2 f}{\partial y^2} \tag{1}$$

However, because the Laplacian measurement operator may change in the x,y directions in the opposite direction, or even cancel each other, so when processing texture images, this phenomenon occurs frequently, which will lead to the instability of the Laplacian operator. Case. To solve this problem, you can rewrite the Laplce operator as (Modifed-Laplce) operator:

$$G(x,y) = \left|\frac{\partial^2 f(x,y)}{\partial x^2}\right| + \left|\frac{\partial^2 f(x,y)}{\partial y^2}\right| \tag{2}$$

In this way, the value of the image sharpness calculated by the improved Laplce operator is equal to or greater than the value of the image sharpness calculated by the original operator. For digital images, the Laplce operator primitive cannot be directly applied, and the primitive must be discretized. Therefore, the improved Laplce operator can be characterized by equation (3) [8].

$$ML(x,y) = |2f(x,y) - f(x-1,y) - f(x+1,y) + |2f(x,y) - f(x,y-1)| \tag{3}$$

In a focused image, the edges of the image are often small. For most non-edge pixels, the gradient value is very small. Therefore, these non-edge points are not suitable for characterizing the sharpness of the image. The conventional method of focusing using image gradients is to simply use the gradient average of the entire image to characterize the sharpness of the image (as shown in Equation 4) [9].

$$ML_{mean} = \frac{\sum_{x=0}^{N-1}\sum_{y=0}^{M-1} ML(x,y)}{M \times N} \tag{4}$$

In the formula, M and N are the number of rows and columns of the image, respectively.

Therefore, this paper proposes an evaluation method of accumulated image sharpness based on the strongest edge gradient Laplacian. The realization mechanism of this method is: to obtain the Laplacian value of each pixel of the image, take the largest of the first P points as the mean T to characterize the sharpness of the image (such as formula 5), usually P takes 50 It can be up to 10.

$$T = \frac{\sum_{i=0}^{i=P-1} MAX_i(ML(x,y))}{P} \tag{5}$$

The design idea of this algorithm: the top P largest Laplacian values used in this algorithm,

because of the small number, it can be basically assumed that the edge with the largest gradient difference in the image plays the most role.

2.2. Precision Positioning Platform and Its Driver

(1) Planar three-degree-of-freedom precision positioning platform

The platform was developed by our laboratory. It is a piezoelectric hinge-driven, flexible hinge-type $XY\theta_z$ precision micro-table that can move in the x and y directions and rotate in a plane around the z axis. The workbench is made by slow wire cutting on an entire metal flat plate according to the design requirements. The selected metal material must have good material properties and elastic properties. This compliant mechanism has outstanding advantages, such as compact mechanism, no gap, small friction, and the same coefficient of thermal expansion in all parts [10-11].

Piezoelectric actuators are used to create micro-displacements through the inverse piezoelectric effect. Piezoelectric ceramics have another strain independent of the direction of the electric field, whose magnitude is proportional to the square of the electric field, called the electrostrictive effect. The deformation formula of piezoelectric ceramics is:

$$S = dE + ME^2 \qquad (6)$$

Where dE is the inverse piezoelectric effect component; ME^2 is the electrostrictive effect component; d is the piezoelectric coefficient (m/V); M is the electrostrictive coefficient (m^4C^2); E is the electric field Strength (V/m); S is strain.

(2) Piezoelectric ceramic controller

The amplifier module is a single-channel power amplifier model XE-505.00. It uses a power amplifier circuit to amplify the weak analog input signal or control signal to meet the driving requirements of piezoelectric ceramics or micro positioning table and other nano positioning mechanisms. Control requirements. According to the characteristics of our laboratory's precision positioning platform, we selected three piezoelectric ceramics [12-13].

2.3. Precision Positioning Process Design

In the focus positioning stage, the scanning probe tip did not contact the sample. The purpose of this stage is to use the optical microscope focusing algorithm to make the relative distance between the probe and the sample to a small order of magnitude, so that the tip of the probe can be brought into contact with the sample quickly during the fine approach [14-15].

In the process of approaching the contact between the traditional probe and the sample, the contact force between the probe and the sample must be adjusted repeatedly to achieve the desired effect, which is not only time-consuming, but also wears on the probe tip. In this paper, the force feedback control technology is used to achieve the precise approach of the probe and the sample. The control effect is good, the wear on the probe tip is small, and it is easy to realize automation [16]. The basic idea is to use the closed-loop feedback mechanism of the AFM scanning control system to adjust the interaction force between the scanning probe and the sample, prevent the sample and the probe from being too strong and damage the probe, and adjust the Z-direction nano platform to the preset Ideal location [17-18].

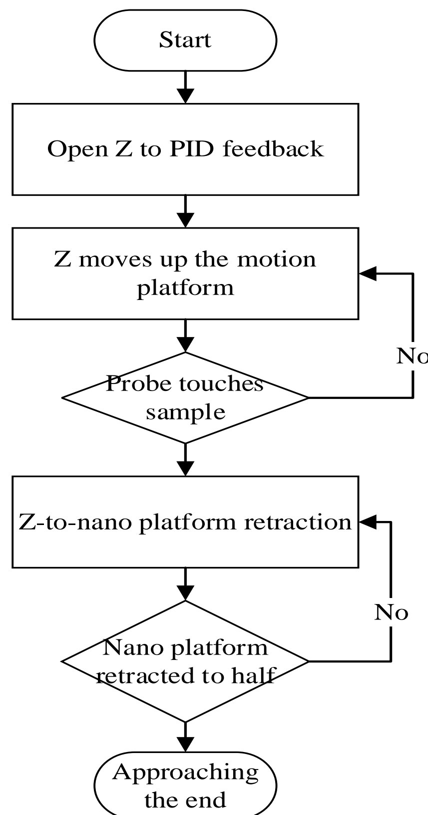

Figure 1. Flow chart of fine approximation

2.4. AFM Probe Tip visual Positioning Technology

The Hough transform was originally used to detect straight lines or line segments in binary maps. Later expanded to other graphics. For line segments in binary maps, Hough linear transformation has high detection accuracy and good robustness [19]. In this paper, the basic principle of Hough linear transformation is mainly used to detect and extract the linear edge of the wafer sample in the optical microscope field of view, so as to obtain the accurate position of the wafer sample edge [20]. Hough line transformation is to use the duality of the point in the image space and the straight line in the parameter space to convert the point in the image space into a straight line in the parameter space, and then convert it into a sinusoidal curve in the polar coordinate system to realize the image space The duality between the point in and the sine curve in the polar coordinate system. The points on the same straight line in the image space have a unique intersection point on the sine curve corresponding to the polar coordinate system [21-22].

Describe the image space as a Cartesian coordinate system, then the equation of the straight line in it can be expressed as:

$$y = kx + p \tag{7}$$

All points (x, y) on this straight line satisfy the above formula. For any point A(x1, y1), if k is transformed into an independent variable, p is transformed into a dependent variable. Then the original form becomes:

$$p = -x_1 k + y_1 \tag{8}$$

Obtain a straight line in the K-P plane, where the slope is $-x_1$ and the intercept is y_1.

2.5. Monocular Visual Electronic Positioning Technology

(1) Distortion correction and calibration

For the positioning of monocular vision, due to the larger area of the projection screen, the distortion of the picture taken by the camera will be more serious. At the same time, because of the difference in the performance of the image acquisition device and the change in the position of the camera, the image will be distorted. Therefore, the distortion of the image needs to be corrected to restore the ideal scene and shape [23-24]. In daily actual image processing, due to different shooting angles, lens and camera distortions will cause changes in the spatial relationship between pixels, which will distort the image, resulting in differences between actual objects and images. Therefore, a suitable and fast camera calibration method is very important to improve the accuracy and real-time performance of the system.

This article uses the calibration procedure of OpenCV to find the internal parameters of the camera, and then corrects them according to the internal parameters to eliminate part of the distortion. Finally, the corner correction and spatial transformation are performed by affine transformation.

(2) Camera calibration

The point on the video image captured by the camera is actually the projected point of the three-dimensional point of the observed actual object on the two-dimensional image coordinate system. The relationship between the point of the space object and the projection point on the two-dimensional plane, that is, the relationship between the three-dimensional position of the object and the two-dimensional coordinates of the corresponding point on the image, depends on the geometric parameter model of the camera. Called the camera parameters. The camera calibration process is the process of obtaining these camera parameters through experiments and calculations [25]. The parameters of the camera include internal and external parameters. Internal parameters refer to the geometric and optical parameters of the camera, mainly including focal length, feature ratio, principal point, distortion factor, etc. The external parameters refer to the rigid motion of the object rotating around the camera or the motion of the camera relative to a fixed scene, which can be referred to as rotation parameters and translation parameters, respectively.

(3) Image denoising

Image denoising is to filter the video image to remove noise, which is image enhancement, smoothing and sharpening. Therefore, the image effect is improved, which is beneficial to the subsequent image analysis work.

Image noise is the random interference signal that an image is subjected to when it is input or transmitted. In video images, sensor noise is the main source of noise. There are two main types of noise: white noise and salt and pepper noise. White noise, also known as Gaussian noise, is a random interference signal in the usual sense. Because its distribution follows the Gaussian distribution, it is called Gaussian noise. At present, there are two main types of filtering and denoising: spatial domain filtering and frequency domain filtering. Spatial domain filtering mainly includes neighborhood average method, median filtering method, histogram filtering and so on. Frequency domain filtering mainly includes three-frame time domain filtering. Spatial domain filtering is often used to eliminate sensor noise, and frequency domain filtering is often used to eliminate scene instantaneous environmental noise. Considering the real-time requirement of this system, the spatial domain filtering is used to eliminate image noise.

In this paper, a 5×5 window median filtering method is used. The following mainly introduces the median filtering method. Before introducing the median filtering method, we must first introduce the concept of windows in digital images. The neighborhood of a certain length or shape of a pixel in an image is called a window. Windows are used in image filtering, image sharpening

and other processes.

2.6. Principal Point Coordinate Calibration

In the linear camera model, the straight line perpendicular to the image plane passing through the camera's perspective center is the focal point, which is called the optical axis. The intersection of the optical axis and the image plane is the principal point. The origins of the camera coordinate system and image coordinate system in the camera model are established on the perspective center and the principal point, respectively. In the process of the coordinate transmission of the spatial point from the camera coordinate system to the image coordinate system, its projection imaging and distortion correction are all based on the collinear geometric relationship formed by the principal point, the perspective center and the optical axis. The accuracy of the main point coordinate calibration has a great influence on the binocular microscope vision system. This paper draws on the method of obtaining the position of the main point using a monocular microscope, and uses the variable magnification method to calibrate the main point of the camera.

Due to the weak perspective of the microscope, it is not feasible to obtain the camera's principal point through the constraint calculation between the image planes. Considering that the principal point is actually the intersection of the optical axis and the CDD imaging surface, and the position of the optical axis is actually unchanged when the microscope magnification changes, so the coordinates of the camera's principal point always remain the same. In other words, for thousands of spatial points projected on the image plane, when the magnification becomes larger or smaller, only the spatial point with the projection position at the main point, the position of the corresponding image point can be maintained Unchanged, the changes in the positions of other points formally expand or contract from the main point.

2.7. Micro Vision Positioning System Construction

(1) Calibration board

Almost all calibration methods require a calibration board or calibration block. The grading table usually has three patterns of dot, square and checkerboard, and the position information of the characteristic pattern can be extracted from these patterns through a specific image extraction technique. Considering that the field of view of the stereo microscope is less than 20 mm, this paper uses a CG-050-T-0.5 glass substrate calibration plate. The square size of this type of calibration plate is 0.5 mm $\times$ 0.5 mm, the total width of the checkerboard pattern is 51 mm $\times$ 51 mm, and the manufacturing accuracy is 1um, which can meet the needs of stereo microscope calibration.

When performing a stereo microscope calibration experiment, images of the calibration plate must be obtained at different positions and at different angles. At the same time, in microscopic vision experiments, the sample must be translated and rotated in different directions and angles. In order to achieve this goal, this paper chose the Zollihan photoelectric control displacement platform to achieve the translational movement of the calibration plate and the sample, and the photoelectric control rotary platform to achieve the degree of rotation and direction of the plate.

(2) Kalman filter

The Kalman filtering method uses a retrospective method, which is a development of Wiener filtering theory and is used to solve the problem of linear filters with different data. The advantage of the Kalman filter is that because filtering is a retrospective process, it is suitable for real-time monitoring. It can filter in multiple dimensions and can be used in fixed and non-static processes. But there are disadvantages: the intensity of the parameters of the matching model is the smallest; after changing the moving target, it will cause the loss of the tracking target, and the error will continue to spread.

3. Experimental Research on Positioning of Tiny Electronic Components Based on Microscope and Computer Vision

3.1. Construction of Software Platform

It mainly includes eight functional modules, namely:

(1) PSD signal receiving function and display

The AFM scanning control system is mainly powered by PSD signals. Therefore, the PSD signal must be collected. Before starting the scan, the position of the laser signal reflected from the radius of the cantilever to the PSD must be adjusted. The position information corresponds to the set point value, and the difference is the bending value of the cantilever.

(2) XYZ nano mobile platform control unit

During the scanning and displaying process, moving the nano-mobile platform in the XY direction can move the AFM in the plane direction. Nano-mobile Z platform will automatically adapt to PID.

(3) Receive shift signal and display to the display part of nano mobile platform

The displacement of the platform Z in the direction of nanometer movement reflects the height difference of the sample surface. A set of Z-direction displacement information can be appropriately reduced to obtain surface morphology information of the sample.

(4) Scanning image display unit

During the scanning process, a set of data can be obtained by reading the amount of expansion and contraction of the Z-mobile nano platform, and a set of predefined colors can be used to characterize the surface information of the scanned sample.

(5) Picture test

After testing the target map, it can basically guarantee the accuracy of the system. In order to fully check the accuracy of the measured area between the two points of the target point, and at the same time make the experiment strict and reliable, an arbitrary point correction experiment is proposed. Choose 9 test points arbitrarily in the experiment and make corrections.

3.2. Subject

Taking the three-degree-of-freedom precision positioning platform developed by our laboratory as one of the research objects, it is assumed that the three input terminals of the platform are A, B, and C input terminals, respectively. It is assumed that an input displacement d_i is applied to the A input terminal of the platform, and there is no input displacement at the B and C terminals. The coupling displacement caused by the action of d_i at the B and C input terminals is Δd_j and Δd_k, respectively. The impact can be described as:

$$\begin{cases} \lambda_1 = \frac{\Delta d_j}{d_i} \\ \lambda_2 = \frac{\Delta d_k}{d_i} \end{cases} \tag{9}$$

3.3. Experimental Data Collection Process

During the delicate approach, the PSD signal indicating the deflection of the detector signal beam and the displacement signal of the nanometer Z-axis movement can be verified. Before starting the experiment, please adjust the Kohler lighting. Kohler lighting is the ideal microscopic lighting method. When setting, please use 40x lens to observe and adjust the focus first. Then adjust the diaphragm diaphragm and condenser field seal to the minimum position. If the current situation

is normal, you should see a polygon with clear edges in the field of view at this time. This is the image of the field diaphragm. If it is not a polygon but a circular point, it means that the position of the condenser is incorrect. Move the condenser lens up and down to make the edge of the image of the field diaphragm clearly visible in the field of view. Then use the resolution board to adjust or determine the size of the pixels. Collect about 1000 frames of images on the light field analysis board, and then measure the images to reduce errors, obtain the vertical outline information of the required line pairs on the resolution board, and use rectangular waves to match the description.

4. Research and Analysis of Experimental Positioning of Tiny Electronic Components Based on Microscope and Computer Vision

4.1. Camera Calibration Experiment and Analysis

In the process of obtaining the distortion coefficient, we assume that the optical distortion becomes zero near the optical center, that is, near the center of the image frame. Therefore, we select the calibration plate feature points at the center of the image for calculation and measurement to obtain the ideal object resolution. After obtaining the lens distortion coefficient in the first step, we can bring the measured actual feature point coordinates and these distortion coefficients back to the formula in the subsequent measurement process, and correct the actual coordinates to the ideal coordinates. After obtaining the lens distortion vector and the actual coordinates of the calibration point, and then obtaining the quotient by knowing the physical distance between the calibration points and the corresponding number of pixels, the object resolution of the image in the x and y directions can be calculated. The results are shown in Table 1.

Table 1. Calculation of object resolution

	Calculation of different feature points before correction			Calculation of different calibration points after correction		
	1-2	2-3	1-3	1-2	2-3	1-3
Object resolution in y direction (un/pixel)	2.174	2.102	2.1065	2.221	2.225	2.213
Object resolution in y direction (un/pixel)	2.143	2.103	2.116	2.105	2.163	2.103

From Table 1, we can see that before the correction, the resolution of the object plane in the x y direction between any two feature points is different, but after the correction is almost the same. When the system magnification changes, the object resolution will also be different. The distortion coefficient is for the lens. If the lens of the system is not replaced, the distortion coefficient remains unchanged. Therefore, in the actual measurement process, as long as the optical hardware conditions are not changed, after the distortion coefficient is obtained at one time, the magnification of the entire system can be adjusted according to the actual measurement needs to obtain the best effect. At this time, as long as the resolution of the object plane can be calibrated, the workload of system calibration is greatly reduced and the working efficiency is improved.

4.2. Image Sharpness Evaluation Function

The figure is the focus evaluation function curve of the gradient average value of the entire image of the standard grid sample, the horizontal axis is the image sequence, and the vertical axis is the image sharpness value. Accumulate the focus evaluation function curve for the strongest edge gradient Laplacian of standard grid sample. It can be seen from the figure that, with many edges, both operators can get a good focus evaluation function curve. However, the sharpest point gradient Laplacian evaluation curve peak point sharpness value is 6 times the peak value of the ordinary

algorithm, and the sharpest edge gradient Laplacian evaluation curve peak point sharpness value is 18 times from the focus sharpness value, while the ordinary algorithm is only 14 times. In contrast, the strongest edge gradient Laplacian is more distinguishable. The experimental results are shown in Figure 2.

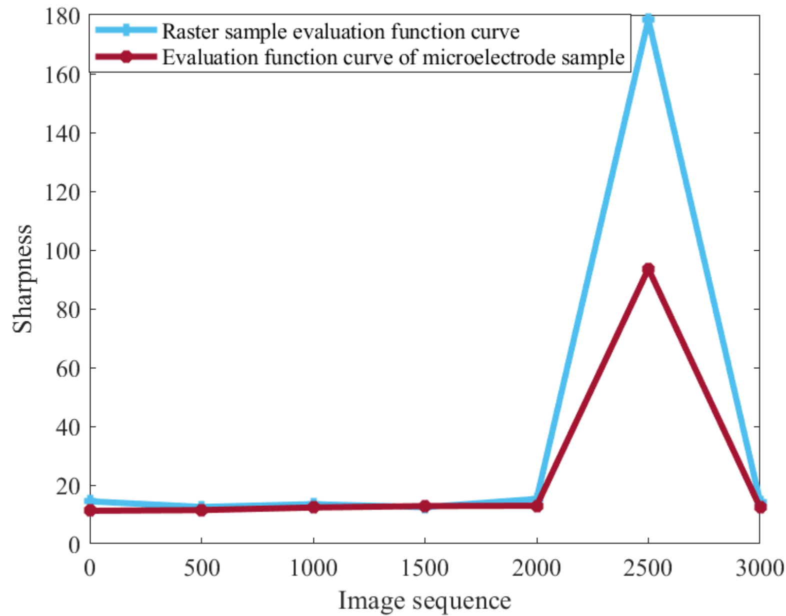

Figure 2. Accumulated focus evaluation function curve of the strongest edge gradient Laplacian of grid and microelectrode samples

Fig. 2 is a gradient evaluation function curve of the average value of the entire image of the microelectrode sample, and Fig. 2 is a cumulative focus evaluation function curve of the strongest edge gradient Laplacian of the microelectrode sample. In the whole image gradient mean algorithm, because there are fewer edges of the microelectrode sample, the gradient change in the focused state will be "averaged" by the value of the non-edge point, so the peak sharpness produced is even better than that of the far focus The peak sharpness of the chip noise is still small, and there are multiple peaks in its evaluation function curve, which cannot be used as the evaluation curve of auto focus. The strongest edge gradient operator can select the edge with the strongest gradient change to participate in the final sharpness value calculation, so it can effectively filter out interference, has a single peak, and meets the requirements of automatic focusing.

4.3. Focal Plane Search Algorithm

The mountain climbing algorithm and the K-cosine algorithm were used to conduct online real-time focusing experiments, respectively, to read the sharpness data of the image in the focusing process, and draw the curve. Since the focus process data is acquired in real time, there is no subsequent node problem. Therefore, in the K-cosine algorithm, the current point is P_{i+k}, the Kth node before the current point is the P_k point, and the 2Kth node before the current point is the P_{i+k} point. K=50 in the experiment. The experimental results are shown in Figure 3.

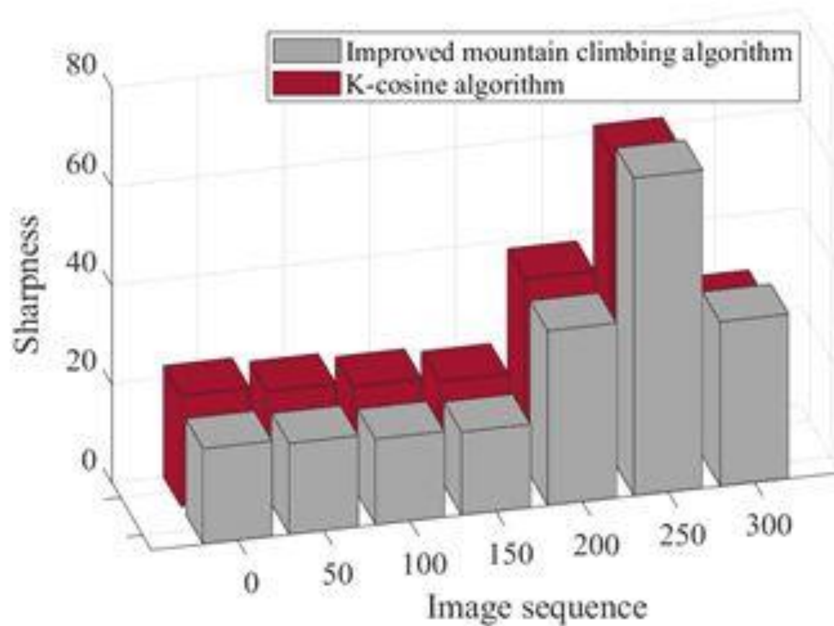

Figure 3. Comparison experiment between improved mountain climbing algorithm and K-cosine algorithm

It can be seen from the figure that both algorithms can effectively identify the peak point. The improved mountain climbing algorithm returns to the peak point after crossing the peak point, and the K-cosine algorithm can directly reach the peak point when K is proper.

4.4. Input Coupling Characteristic Test and Analysis of Precision Positioning Platform

In order to test the effect of coupling displacement between each input end of the planar three-degree-of-freedom micro-movement stage, during the measurement process, first move the two-dimensional worktable so that the fixed camera focus is respectively aligned with the two inputs of the micro-movement stage where no piezoelectric ceramic is installed Table 2 shows the results of coupling analysis of the micro-motion platform obtained through ANSYS simulation and this experiment.

Table 2. Input coupling analysis results

Input coupling	ANSYS simulation value		Visual measurement results	
	λ_1	λ_2	$\overline{\lambda_1}$	$\overline{\lambda_2}$
Numerical value	3.2×10^{-3}	4.4×10^{-3}	3.8×10^{-3}	4.4×10^{-3}

In the same way, the coupling displacement of the B and C input terminals of the input terminal of the precision positioning platform A under other input displacements can be measured separately, and the relationship curve is shown in Figure 4.

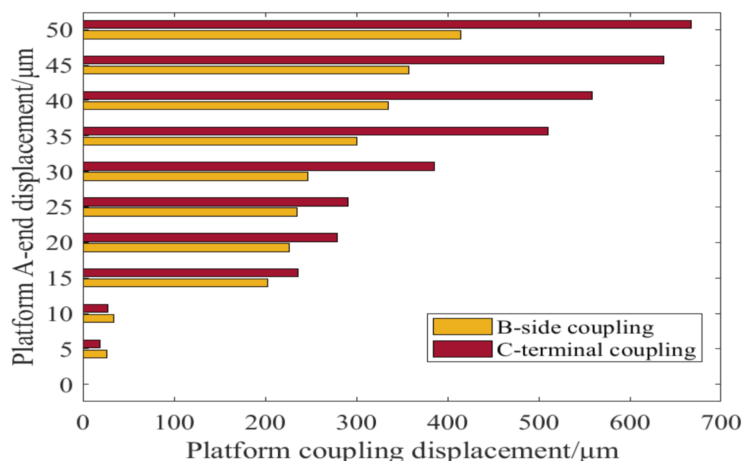

Figure 4. Relationship between input coupling displacement of platform B and C

It can be seen from Figure 4 that the platform still has a large input coupling displacement error, and as the displacement at the input end of the platform increases, the coupling displacement at both ends also increases. Among them, the maximum coupling displacement of the B and C input terminals is about 0.43 microns and 0.67 microns. For a precision positioning platform, such coupling displacement cannot be ignored.

4.5. Analysis of Scanning Probe tip Blind Positioning Method

During the AFM scanning process, the controller adjusts the expansion and contraction of the piezoelectric ceramic in the Z direction, so that the scanning sample and the probe tip are always in the state of van der Waals repulsion, and the interaction force is unchanged. When the surface morphology of the scanned sample changes, the degree of bending of the scanning probe cantilever beam changes, the reflected laser signal deflects, and the PSD output current changes. The controller adjusts the displacement of the Z-axis nano-mobile platform in time according to the PSD signal change, so that the scanning probe can follow the changes in the surface morphology of the sample. As shown in Figure 5, it is a single-line data curve obtained in the X direction when AFM scans a 50 nm standard grid. Among them, the scanning range is 50 um.

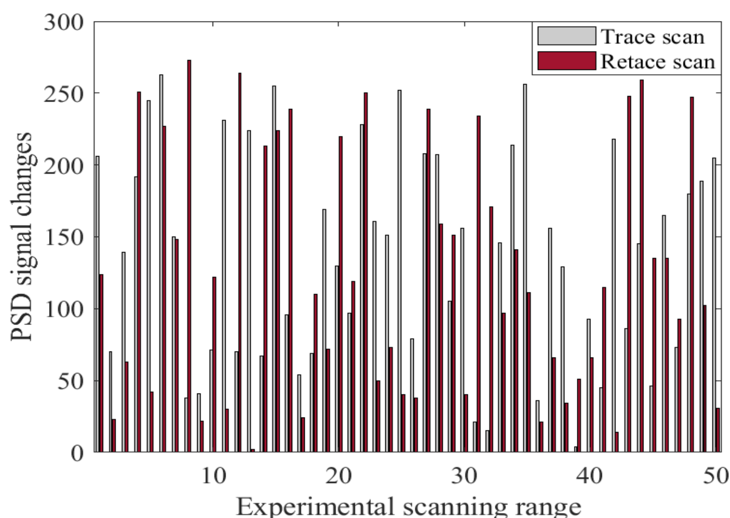

Figure 5. Single-line scan data curve of 50nm standard grid

As shown in Figure 5, during the scanning imaging process of AFM, in order to ensure the scanning accuracy, it is necessary to reciprocate the scanned sample within one scanning cycle, that is, to scan the same sample at the same position from different directions. According to the results of two scans, two trace curves of trace and retace are drawn. The blue curve is the trace curve, and the red curve is the retace curve. In an ideal situation, the two curves roughly coincide.

5. Conclusion

Aiming at the problem of difficulty in capturing the scanning target during the AFM scanning process, this paper proposes a blind calibration method for the scanning probe tip based on the Hough transform and AFM scanning data. In this article, the principle of Hough linear transformation is explained in detail. Through micro-nano manipulation technology, corner detection technology and Hough linear transformation technology, the AFM probe tip is captured in the optical microscope field of view. The coordinate conversion technology in robotics is used to realize the unification of the coordinate system of the macro mobile platform, the coordinate system of the nano mobile platform and the coordinate system of the optical microscope field of view. Use a unified coordinate system to achieve the target position of the sample to be scanned and the positioning of the tip of the AFM probe. This method effectively solves the problem of positioning the scanning probe and the scanning sample on the XY plane, and realizes the accurate scanning of the target position.

In this paper, a computer vision coupled measurement experiment platform is built. Using computer micro vision technology, the non-contact, real-time, high-efficiency and high-precision measurement of the coupled displacement of the platform is realized. Through the image display window, the size and direction of the coupling displacement can be directly observed, which is intuitive. Finally, in view of the input coupling phenomenon existing on the platform itself, the transfer function matrix between the input and output of the platform is modified through experiments to eliminate the influence of the coupling displacement on the positioning accuracy of the platform.

In this paper, focus contrast test was conducted with standard grid samples and microelectrode samples, and it was proved that the improvement of the algorithm improved the algorithm's noise resistance, reliability and stability. The commonly used focus search algorithms are analyzed, and real-time focusing is performed using the hill climbing algorithm and the K-cosine algorithm, respectively. An automatic approach method of the tip of the AFM scanning probe and the sample to be scanned based on computer vision and precise force feedback technology is proposed. This method solves the positioning problem of the AFM scanning probe and the sample to be scanned in the Z direction through coarse and fine segmented positioning. An automatic approximation experiment was carried out with standard grid samples, and the data of the test process was recorded and analyzed and proved, which proved the feasibility of the method. At the same time, the construction of the nano-operation software platform was completed, which has basic nano-operation capabilities.

Funding

This article is not supported by any foundation.

Data Availability

Data sharing is not applicable to this article as no new data were created or analysed in this study.

Conflict of Interest

The author states that this article has no conflict of interest.

References

[1] Han G, Cao S, Wang X, et al. Blind Evaluation of AFM Tip Shape by Using Optical Glass Surface with Irregular Nanostructures as a Tip Characterizer. Micro & Nano Letters, 2017, 12(12):916-919. DOI: 10.1049/mnl.2017.0200

[2] Cao F, Donnarumma F, Murray K K. Wavelength Dependent Atomic Force Microscope Tip-enhanced Laser Ablation. Applied Surface ence, 2018, 447(JUL.31):437-441.

[3] Sharov V A, Dunaevskiy M S, Kryzhanovskaya N V, et al. Light absorption by an atomic force microscope probe. Journal of Physics Conference Series, 2017, 816(1):012036. DOI: 10.1088/1742-6596/816/1/012036

[4] Zhang L, Song Y, Hosoi A, et al. Microwave atomic force microscope: MG63 osteoblast-like cells analysis on nanometer scale. Microsystem Technologies, 2016, 22(3):603-608.

[5] Lu H, Shang W, Xie H, et al. Ultrahigh-Precision Rotational Positioning Under a Microscope: Nanorobotic System, Modeling, Control, and Applications. IEEE Transactions on Robotics, 2018, PP(99):1-11. DOI: 10.1109/TRO.2017.2783937

[6] Shan G, Li Y, Zhang L, et al. Contributed Review: Application of voice coil motors in high-precision positioning stages with large travel ranges. Review of Scientific Instruments, 2015, 86(10):101501.

[7] Mukai K, Hirota A, Shimizu Y, et al. Template method for nano-order positioning and dense packing of quantum dots for optoelectronic device application. Semiconductor Science & Technology, 2015, 30(4):044006.

[8] Hu X, Wan J, Wu S, et al. Fast Positioning Method for Industrial Scanning Probe Microscopy. Nami Jishu Yu Jingmi Gongcheng/nanotechnology & Precision Engineering, 2015, 13(1):8-16.

[9] Tien C L, Lai Q H, Lin C S . Development of optical automatic positioning and wafer defect detection system. Measurement ence & Technology, 2016, 27(2):025205.

[10] Sadeghian H, Herfst R, Winters J, et al. Development of a detachable high speed miniature scanning probe microscope for large area substrates inspection. Review of entific Instruments, 2015, 86(11):12-264.

[11] Kausar A, Reza A, Latef T, et al. Optical Nano Antennas: State of the Art, Scope and Challenges as a Biosensor Along with Human Exposure to Nano-Toxicology. Sensors, 2015, 15(4):8787-8831. DOI: 10.3390/s150408787

[12] Eisenstein M . Super-resolve me: from micro to nano. Nature, 2015, 526(7573):459.

[13] Cui J, Yang L, Wang Y, et al. Nanospot Soldering Polystyrene Nanoparticles with an Optical Fiber Probe Laser Irradiating a Metallic AFM Probe Based on the Near-Field Enhancement Effect. Acs Applied Materials & Interfaces, 2015, 7(4):2294-2300.

[14] Sriramshankar R, Sri M M R, Jayanth G R . Design and fabrication of a flexural harmonic AFM probe with an exchangeable tip. Journal of Micro-Bio Robotics, 2017, 13(1-4):1-15. DOI: 10.1007/s12213-017-0100-z

[15] Mishina K, Miura Y, Kawashima K, et al. Si Nano-tip Sharpening and Fabrication of Narrow-gapped Dual AFM Probe. IEEJ Transactions on Sensors and Micromachines, 2016, 136(7):312-318.

[16] Keatley P S, Loughran T H J, Hendry E, et al. A platform for time-resolved scanning Kerr microscopy in the near-field. Review of Scientific Instruments, 2017, 88(12):123708. DOI: 10.1063/1.4998016

[17] Camci, Fatih. Maintenance scheduling of geographically distributed assets with prognostics

information. European Journal of Operational Research, 2015, 245(2):506-516.

[18] Pham K N, Ta K H T, Nguyen L T T, et al. Surface Mapping of Resistive Switching CrO x Thin Films. Advances in Materials Physics & Chemistry, 2016, 06(3):21-27.

[19] Mahapatra P K, Sethi S, Kumar A. Comparison of Artificial Immune System and Particle Swarm Optimization Techniques for Error Optimization of Machine Vision Based Tool Movements. Journal of the Institution of Engineers, 2015, 96(4):363-372.

[20] Y. Liu, Q. Xu. Design of a flexure-based auto-focusing device for a microscope. International Journal of Precision Engineering and Manufacturing, 2015, 16(11):2271-2279.

[21] Corinne E. Isaac, Elizabeth A. Curley, Paméla T. Nasr. Cryogenic positioning and alignment with micrometer precision in a magnetic resonance force microscope. Review of entific Instruments, 2018, 89(1):013707.

[22] Sri M M R, Sriramshankar R, Jayanth G R. Direct Measurement of Three-Dimensional Forces in Atomic Force Microscopy. IEEE/ASME Transactions on Mechatronics, 2015, 20(5):2184-2193.

[23] Solina, Franc. Volumetric models in computer vision: an overview. Journal of Computing & Information Technology, 2015, 2(3):155-166.

[24] Constant false alarm rate algorithm in infrared focal plane array rotation search system. Infrared and Laser Engineering, 2016, 45(2):204003.

[25] Chan K G, Michael L. Direct inversion algorithm for focal plane scanning optical projection tomography. Biomedical Optics Express, 2017, 8(11):5349-5355.